

Tuning the Nanocellulose–Borate Interaction To Achieve Highly Flame Retardant Hybrid Materials

Bernd Wicklein,^{*,†,‡} Darko Kocjan,[‡] Federico Carosio,[§] Giovanni Camino,[§] and Lennart Bergström^{*,†}

[†]Department of Materials and Environmental Chemistry, Stockholm University, Svante Arrheniusv. 16C, 106 91 Stockholm, Sweden

[‡]Laboratory of Biomolecular Structure, National Institute of Chemistry, CoE ENFIST, Hajdrihova 19, 1000 Ljubljana, Slovenia

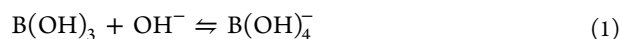
[§]Dipartimento di Scienza Applicata e Tecnologia, Politecnico di Torino – Sede di Alessandria, V.le Teresa Michel, 5, 15121 Alessandria, Italy

S Supporting Information

Commercial use of (bio)polymer-based materials in, e.g., insulating and building applications requires a high degree of flame retardancy.¹ Flame retardant polymer-based materials are commonly produced by blending the polymer matrix with appropriate additives and fillers including nanofillers,² e.g., clays or silica and alumina nanoparticles.^{3,4} Boric acid is one of the most frequently used flame retardants for cellulosic materials including fabrics and wood^{5,6} and acts by providing a glass-like coating on the fire exposed surface² and by promoting polymer dehydration and char formation.^{2,7}

Polymer degradation and char formation is a complex process being influenced not only by the specific reactions and complexes that boric acid may have formed with the polymer matrix during preparation but also by in situ reactions of boric acid with the polymer during thermal exposure and combustion.² Such reactions may lead to polymer cross-linking, which is known to improve char formation by cyclization and condensation.⁸ Even though previous work has shown that boric acid can form ester bonds with polyols⁹ and anhydrides with carboxylic acid groups,¹⁰ the thermal aspects of these reactions and how such in situ reactions may improve the flame retardancy are poorly understood.

The complexation of boric acid and/or borate anions with a polymer is pH dependent¹¹ since boric acid (BA) exists in equilibrium with the borate (B) anion according to eq 1,



Below the pK_a of boric acid (9.2),¹² BA is mainly present while above pH 9.2, B(OH)_4^- ions, B, are dominant. The predominance of either boric acid or borate anions may greatly influence the structure and properties of polymer–borate/boric acid hybrids.^{9,13} For instance, borate anions react with the alcoholic groups of carbohydrates and form mono- or bis-chelate esters through the complexation with diols,¹⁴ while boric acid preferably reacts with carboxyl and amine groups.¹⁰ These pH-dependent reaction paths are poorly understood for cellulose, and little is known about how the pH-dependent complexations determine the flame retardancy.

Here, we have studied the pH-dependent complexation of boric acid (BA) and borate (B) with cellulose nanofibers (CNF) and the effects on flame retardancy. Cellulose nanofibers¹⁵ are an emerging nanomaterial with interest in several areas of technological importance^{16,17} including sustainable and renewable superinsulating materials.¹⁸ The boron–CNF interactions have been examined by solid-state ¹¹B

MAS NMR spectroscopy combined with molecular modeling. In addition, we evaluated the combined effect of boric acid or borate together with sepiolite nanoclay on the thermal stability including combustion resistance of CNF-based composite foams. Sepiolite is a needle-like magnesium silicate used in mechanical reinforcement of polymer nanocomposites¹⁹ and shows good flame retardant properties.¹⁸

We have investigated the chemistry of CNF–BA–SEP and CNF–B–SEP hybrids prepared at pH 7 and pH 10, respectively, by ¹¹B MAS NMR. Figure 1a shows that the spectrum for a CNF–BA–SEP complex prepared at pH 7 is dominated by the signal at 18 ppm, which is attributed to unreacted trigonal boric acid B(OH)_3 , while the spectrum for the CNF–B–SEP complex prepared at pH 10 is dominated by the signals at 6 and at 2 ppm, corresponding to tetragonal (anionic) borate bis-chelate L–B–L (where L denote CNF as a ligand) and to unreacted borate anion B and monochelate L–B,²⁰ respectively. Deconvolution of the ¹¹B MAS NMR signals suggests a consumption of boric acid at both pH values as it undergoes a complexation reaction with CNF (Table S1).¹⁴ We find that the degree of cross-linking, i.e., the relative concentration of [L–B–L] versus [L–B], is pH dependent and increases from 0.06 at pH 7 to 0.17 at pH 10. The enhanced cross-linking at alkaline pH is also corroborated by the formation of a viscoelastic CNF gel with a 6-fold higher storage modulus at pH 10 compared to pH 7 (Figure S1).

The similarity of the ¹¹B MAS NMR spectra of CNF–BA and CNF–BA–SEP (Figure S2) suggests that sepiolite (SEP) has no major influence on the CNF–BA complexation. However, IR and ²⁹Si CP/MAS NMR measurements (Figure S3) suggest that sepiolite may interact with boric acid and/or borate via H-bonding and form covalent bonds at both pH 7 and 10.²¹ Hence, the molecular structure of CNF–BA–SEP involves chemical C–O–B and Si–O–B bonds and possibly hybrid organic/inorganic links of cellulose fibers and sepiolite nanoparticles via boron moiety bridging (C–O–B–O–Si).

The flame retardancy was assessed by cone calorimetry tests on $5 \times 5 \text{ cm}^2$ foam panels of CNF–BA/B–SEP hybrids with a composition of 54/11/35 wt % of CNF, BA or B, and SEP, respectively. Figure 1b shows that the hybrid prepared at pH 10

Received: February 6, 2016

Revised: March 21, 2016

Published: March 21, 2016

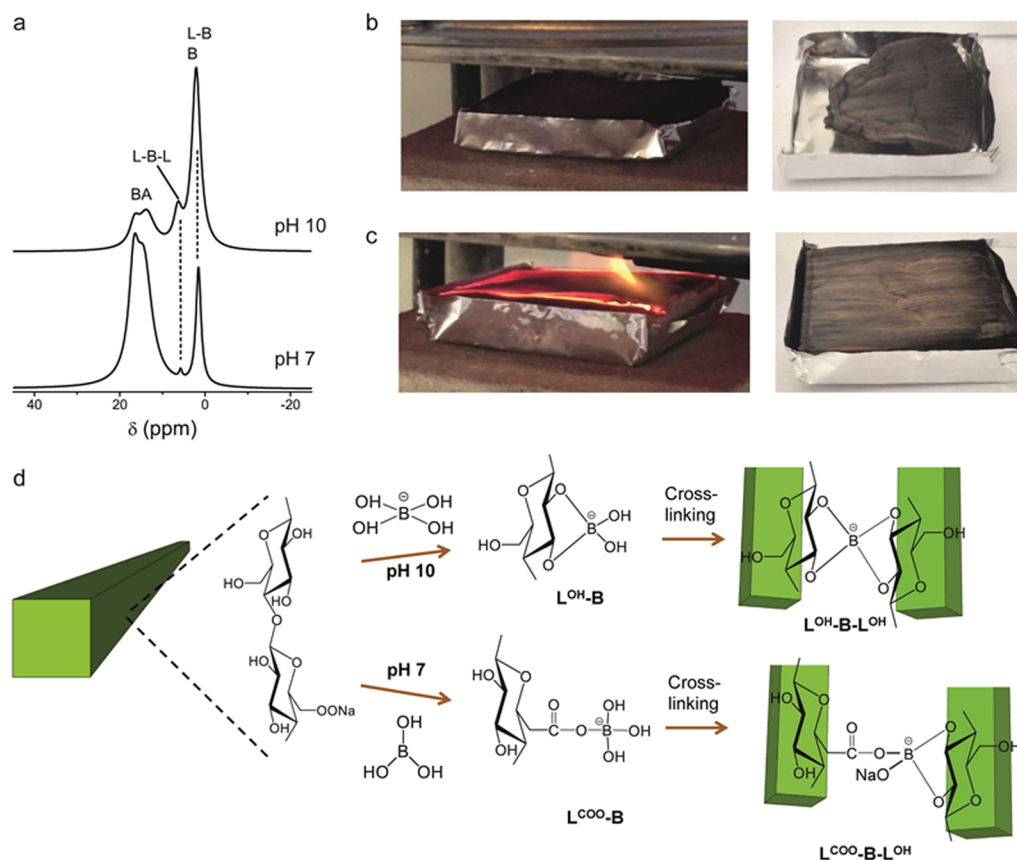


Figure 1. Complex formation and fire retardancy of cellulose nanofiber (CNF) and boric acid (BA)/borate (B) materials with added sepiolite (SEP). (a) ^{11}B MAS NMR spectra of CNF-11%BA-35%SEP and CNF-11%B-35%SEP hybrids prepared at pH 7 and at pH 10, respectively. Photographs taken during cone calorimetry tests and of the respective residues of (b) CNF-11%B-35%SEP hybrid prepared at pH 10 and (c) CNF-11%BA-35%SEP hybrid prepared at pH 7. (d) Schematic representation of the molecular pathway of the BA complexation with the hydroxyl and carboxylic functional groups on CNF at neutral and alkaline conditions.

does not ignite, undergoing only flameless pyrolysis, while the hybrid prepared at pH 7 ignites but self-extinguishes after a few seconds (Figure 1c). The peak of heat release rate (pkHRR) of the hybrid prepared at pH 10 is below the instrumental detection limit while the pkHRR of the hybrid prepared at pH 7 is only $20 \pm 1 \text{ kW m}^{-2}$. For comparison, commercially available flame resistant phenolic foams have typically pkHRR values in the range of $70\text{--}100 \text{ kW m}^{-2}$.²² Hence, the high degree of CNF esterification at pH 10 has a remarkable effect on the flame resistance behavior of the CNF-B-SEP hybrid. Moreover, the pore and wall microstructure of the CNF-B-SEP foam is maintained after the combustion test and shows no signs of collapse (Figure S4). For comparison, pure CNF and CNF-40 wt % SEP foam panels were also tested and both samples ignited (Figure S5) with pkHRR values of $60 \pm 8 \text{ kW m}^{-2}$ and $59 \pm 9 \text{ kW m}^{-2}$, respectively. The CNF foam was completely combusted while the CNF-SEP foam panel was partially preserved.

Figure 1 shows that the complexation of boric acid or borate with the diols on CNF is strongly influenced by pH-dependent speciation of the reactive $\text{B}(\text{OH})_4^-$ anion and that the difference in molecular architecture has a large effect on the flame retardancy of the CNF-BA/B-SEP hybrid foam panels. The molecular pathway shown in Figure 1d suggests that the dominating cross-linking reaction at pH 10 involves the formation of a bis-chelate $\text{L}^{\text{OH}}\text{-B-L}^{\text{OH}}$ complex of the borate anion with the C2,3-diol on the CNF. The specific pathways

given in Figure 1d are supported by molecular modeling, where the lowest potential energy for the $\text{L}^{\text{OH}}\text{-B}$ and $\text{L}^{\text{OH}}\text{-B-L}^{\text{OH}}$ configurations was calculated as -1175 au and -1709 au , respectively (cf. Supporting Information discussion and Figure S6).

Boric acid does not complex with diols at neutral pH but may react with the carboxylate groups^{14,23} that are present on the surface of the TEMPO-mediated oxidized cellulose nanofibers²⁴ used in this work (cf. Figure 1d). Molecular modeling suggests the formation of a carboxylate anhydride $\text{L}^{\text{COO}}\text{-B}$ with a potential energy about 30 kcal/mol lower than that of $\text{L}^{\text{OH}}\text{-B}$ (Table S2). Indeed, the anhydride reaction is supported by the appearance of the carbonyl IR band at 1725 cm^{-1} and the simultaneous decrease of the COO^- band intensity in the IR spectra (Figure S7). However, ^{11}B MAS NMR spectra show that the relative number of carboxylate esters at pH 7 is smaller than diol-borate complexes at pH 10 (cf. Figure 1a and Table S1), which probably is related to the 5-fold lower availability of carboxylate groups compared to surface C2,3-diols. Therefore, the formation of a diol-borate chelate $\text{L}^{\text{COO}}\text{-B-L}^{\text{OH}}$ with a second fiber at pH 7 is not so probable given the relative scarcity of reactive carboxylate esters.

CNF-BA hybrids have been investigated by a combination of thermal analysis and solid state ^{11}B and ^{13}C NMR of thermally annealed samples to determine the chemical transformations during combustion. The weight loss results in nitrogen show a residual weight at $800 \text{ }^\circ\text{C}$ that is about 31 wt %

higher for the 60/40 (w/w) CNF–BA hybrid prepared at pH 7 (Figure 2a), compared to the sum of the residues of the

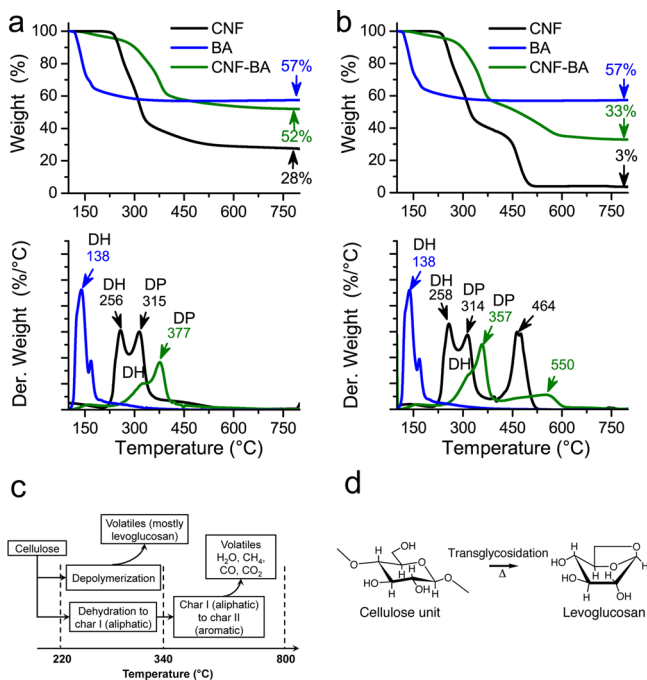


Figure 2. Thermogravimetric analysis in (a) nitrogen and (b) air of neat CNF, neat BA, and a 60/40 (w/w) CNF–BA complex prepared at pH 7. DH denotes dehydration and DP denotes depolymerization. (c) Schematic representation of cellulose pyrolysis steps and cellulose degradation to levoglucosan. (d) Transglycosidation of levoglucosan in a “boat” conformation from cellulose in a “chair” conformation.

individual components (BA and CNF). The amount of organic residue (i.e., char) produced from CNF–BA hybrids is increased by 70 wt % as compared to pristine CNF, which implies that as much as 50 wt % of CNF is transformed into char when complexed with BA. The major weight loss (about 60 wt %, between 220 and 340 °C) of CNF involves two partially overlapping processes with maximum rates at 256 and 315 °C, respectively (Figure 2a). The first process is related to intra- and intermolecular water elimination resulting in “anhydrocellulose”, while the second process involves depolymerization and formation of volatile levoglucosan (Figure 2c).^{6,25} The thermal degradation of the CNF–BA hybrid displays a dehydration step that is significantly smaller than the subsequent depolymerization step. Additionally, the weight loss from thermal degradation of CNF in the hybrid is shifted to a temperature that is about 80 °C higher compared to pure CNF. This temperature shift is probably due to a reduction of the concentration and availability of reactive OH groups in the CNF–BA hybrid. The TG results also show that the maximum rate of depolymerization and volatilization of BA cross-linked CNF is 50% lower compared with pure CNF, which suggests that the formation of the volatile and combustible levoglucosan is less abrupt in the CNF–BA hybrids. The intramolecular transglycosidation reaction that leads to levoglucosan has been linked to a chair to boat conformation change (Figure 2d),⁷ which may be hindered by boron cross-linking (see Figure 1d). In air, comparison of the weight loss of pure CNF and CNF–BA hybrid (Figure 2b) suggests that the presence of a boric anhydride may slow down char oxidation and shifts it to higher temperatures (464 to 550 °C).

CNF–BA hybrids have also been thermally annealed in nitrogen because anaerobic polymer thermal degradation processes also are important in combustion.⁷ With guidance from the thermogravimetry data, thermal annealing a CNF–BA hybrid at 180 and 450 °C should relate to a state before and after char formation. The ¹¹B MAS NMR data in Figure 3a

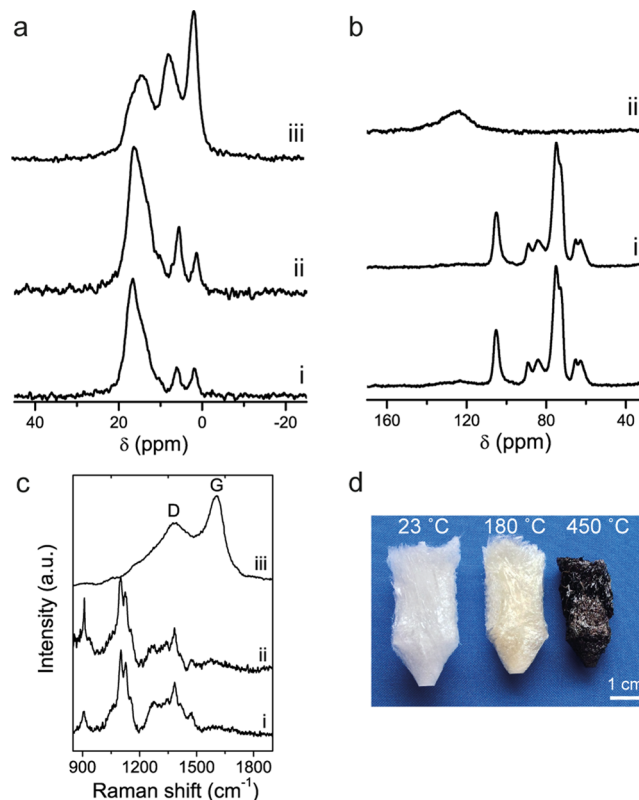


Figure 3. (a) ¹¹B MAS NMR, (b) ¹³C CP/MAS NMR, and (c) Raman spectra of CNF–2.4 wt % BA hybrids; (i) as prepared at pH 7 and annealed under N₂ at (ii) 180 °C, and (iii) 450 °C, respectively. (d) Photographs of the respective materials.

show that the borate signals of the monochelate, B–L, and bis-chelate, L–B–L, at 1.5 and 7.5 ppm, respectively, increase significantly, while the signal of unreacted boric acid (at 14 ppm) decreases with increasing temperature up to 450 °C. Quantification of the signals suggests that unreacted BA is consumed as it undergoes an esterification reaction with CNF leading to an increase of the degree of esterification of CNF from 2.5 to 12.2% when the temperature is increased from room temperature to 450 °C (Table S1). The degree of esterification refers to the ratio of accessible surface C2,3-diols in a 6 × 6 cellulose Iβ model of CNF²⁶ that are complexed by borate anions. Importantly, also the ratio of cross-linked [L–B–L] complexes versus monochelate [L–B] complexes increases with temperature by 23%, suggesting that CNF undergoes a thermally induced esterification/cross-linking process. Indeed, this is in agreement with the observed increase of CNF charring in thermal degradation of cross-linked CNF–BA hybrids as shown by TGA (cf. Figure 2). The ¹³C CP/MAS NMR spectrum of the CNF–2.4 wt % BA hybrids during annealing in Figure 3b indicates complete transformation of the polysaccharide into a graphitized structure at 450 °C, where the broad peak between 120 and 100 ppm is attributed to sp² C atoms. This graphitization is also corroborated by the Raman

spectra in Figure 3c, where an intense G band around 1608 cm^{-1} (sp^2 carbon) appears for the hybrid annealed at 450 °C, while at the same time the typical cellulose bands at 900 and 1100 cm^{-1} , respectively, disappear. The aromatization of annealed hybrids is also confirmed by IR (Figure S8). Figure 3d shows that CNF–BA hybrid foams become black but maintain their porous structure during the annealing process.

In summary, we have investigated the chemistry of the pH-dependent cross-linking of boric acid or borate anions with nanocellulose with solid state NMR and shown that the molecular pathway at neutral and alkaline conditions influences strongly the flame retardancy and ignition resistance. The pH-dependent speciation of boric acid into borate anions at high pH and the different reactivity of boric acid and borate anion toward the diol and carboxylic acid functional groups on the nanocellulose backbone control the molecular cross-linking pathways. Thermal analysis shows that char oxidation is slowed down and shifted to higher temperatures and that the formation of the volatile and combustible levoglucosan is less abrupt in the CNF–borate hybrids compared to CNF that has not been cross-linked. Analysis of the thermally annealed residues by a combination of ^{11}B MAS and ^{13}C CP/MAS NMR, Raman, and infrared spectroscopy shows that the formation of a CNF–borate hybrid promotes charring and complete transformation of the polysaccharide at 450 °C into a graphitized structure. Preparation of freeze-cast foams from nanocellulose–borate hybrids with the addition of sepiolite clay results in complete suppression of polymer ignition on radiant heat exposure. The ability to strongly reduce the flammability of nanocellulose hybrid foams is important for the development of, e.g., sustainable and eco-friendly thermal insulation materials.

■ ASSOCIATED CONTENT

Supporting Information

The Supporting Information is available free of charge on the ACS Publications website at DOI: 10.1021/acs.chemmater.6b00564.

Experimental details, solid-state NMR, IR, rheological, and molecular modeling data, respectively, and SEM images of CNF–BA hybrids (PDF)

■ AUTHOR INFORMATION

Corresponding Authors

*B. Wicklein, E-mail: bernd@icmm.csic.es.

*L. Bergström, E-mail: lennart.bergstrom@mmk.su.se.

Present Address

#B. Wicklein: Materials Science Institute of Madrid, 28049 Madrid, Spain

Notes

The authors declare no competing financial interest.

■ ACKNOWLEDGMENTS

Financial support from the Swedish Strategic Foundation (SSF, RMA11-0065) and the Swedish Energy Agency (STEM, 40121-1) is acknowledged. B.W. acknowledges financial support from CICYT (Spain, project MAT2012-31759) and the COST Action MP1202. The authors thank Prof. Salazar-Alvarez for fruitful discussions.

■ REFERENCES

- (1) Cho, J. H.; Vasagar, V.; Shanmuganathan, K.; Jones, A. R.; Nazarenko, S.; Ellison, C. J. Bioinspired Catecholic Flame Retardant Nanocoating for Flexible Polyurethane Foams. *Chem. Mater.* **2015**, *27*, 6784–6790.
- (2) Dasari, A.; Yu, Z. Z.; Cai, G. P.; Mai, Y. W. Recent developments in the fire retardancy of polymeric materials. *Prog. Polym. Sci.* **2013**, *38*, 1357–1387.
- (3) Li, Y.; Schulz, J.; Mannen, S.; Delhom, C.; Condon, B.; Chang, S.; Zapparano, M.; Grunlan, J. C. Flame Retardant Behavior of Polyelectrolyte-Clay Thin Film. *ACS Nano* **2010**, *4*, 3325–3337.
- (4) Chen, S.; Li, X.; Li, Y.; Sun, J. Intumescent Flame-Retardant and Coatings on Cotton Fabric. *ACS Nano* **2015**, *9*, 4070–4076.
- (5) Horrocks, A. R. Flame retardant challenges for textiles and fibres: New chemistry versus innovatory solutions. *Polym. Degrad. Stab.* **2011**, *96*, 377–392.
- (6) Alongi, J.; Malucelli, G. Cotton flame retardancy: State of the art and future perspectives. *RSC Adv.* **2015**, *5*, 24239–24263.
- (7) Kandola, B. K.; Horrocks, A. R.; Price, D.; Coleman, G. V. Flame-Retardant Treatments of Cellulose and Their Influence on the Mechanism of Cellulose Pyrolysis. *J. Macromol. Sci., Polym. Rev.* **1996**, *36*, 721–794.
- (8) Di Blasi, C.; Branca, C.; Galgano, A. Flame retarding of wood by impregnation with boric acid - Pyrolysis products and char oxidation rates. *Polym. Degrad. Stab.* **2007**, *92*, 752–764.
- (9) Rietjens, M.; Steenbergen, P. A. Crosslinking mechanism of boric acid with diols revisited. *Eur. J. Inorg. Chem.* **2005**, *2005*, 1162–1174.
- (10) Lundberg, H.; Tinnis, F.; Selander, N.; Adolffson, H. Catalytic amide formation from non-activated carboxylic acids and amines. *Chem. Soc. Rev.* **2014**, *43*, 2714–2742.
- (11) Yoshimura, K.; Miyazaki, Y.; Ota, F.; Matsuoka, S.; Sakashita, H. Complexation of boric acid with the N-methyl-D-glucamine group in solution and in crosslinked polymer. *J. Chem. Soc., Faraday Trans.* **1998**, *94*, 683–689.
- (12) Momii, R. K.; Nachtrieb, N. H. Nuclear magnetic resonance study of borate-polyborate equilibria in aqueous solution. *Inorg. Chem.* **1967**, *6*, 1189–1192.
- (13) Audebeau, E.; Oikonomou, E. K.; Norvez, S.; Iliopoulos, I. One-pot synthesis and gelation by borax of glycopolymers in water. *Polym. Chem.* **2014**, *5*, 2273–2281.
- (14) Peters, J. A. Interactions between boric acid derivatives and saccharides in aqueous media: Structures and stabilities of resulting esters. *Coord. Chem. Rev.* **2014**, *268*, 1–22.
- (15) Moon, R. J.; Martini, A.; Nairn, J.; Simonsen, J.; Youngblood, J. Cellulose nanomaterials review: Structure, properties and nanocomposites. *Chem. Soc. Rev.* **2011**, *40*, 3941–3994.
- (16) Li, S.; Huang, J. Cellulose-Rich Nanofiber-Based Functional Nanoarchitectures. *Adv. Mater.* **2016**, *28*, 1143–1158.
- (17) Zhang, Z.; Sebe, G.; Rentsch, D.; Zimmermann, T.; Tingaut, P. Ultralightweight and Flexible Silylated Nanocellulose Sponges for the Selective Removal of Oil from Water. *Chem. Mater.* **2014**, *26*, 2659–2668.
- (18) Wicklein, B.; Kocjan, A.; Salazar-Alvarez, G.; Carosio, F.; Camino, G.; Antonietti, M.; Bergström, L. Thermally insulating and fire-retardant lightweight anisotropic foams based on nanocellulose and graphene oxide. *Nat. Nanotechnol.* **2015**, *10*, 277–283.
- (19) Ruiz-Hitzky, E.; Darder, M.; Fernandes, F. M.; Wicklein, B.; Alcántara, A. C. S.; Aranda, P. Fibrous clays based bionanocomposites. *Prog. Polym. Sci.* **2013**, *38*, 1392–1414.
- (20) Bishop, M.; Shahid, N.; Yang, J.; Barron, A. R. Determination of the mode and efficacy of the cross-linking of guar by borate using MAS 11B NMR of borate cross-linked guar in combination with solution 11B NMR of model systems. *Dalt. Trans.* **2004**, *17*, 2621–2634.
- (21) Wicklein, B.; Aranda, P.; Ruiz-Hitzky, E.; Darder, M. Hierarchically structured bioactive foams based on polyvinyl alcohol–sepiolite nanocomposites. *J. Mater. Chem. B* **2013**, *1*, 2911–2920.
- (22) Hu, X.-M.; Zhao, Y.-Y.; Cheng, W.-M. Effect of Formaldehyde/Phenol Ratio(F/P) on the Properties of Phenolic Resins and Foams

Synthesized at Room Temperature. *Polym. Compos.* **2015**, *36*, 1531–1540.

(23) Köse, D. A.; Zümreoglu-Karan, B. Mixed-ligand complexes of boric acid with organic biomolecules. *Chem. Pap.* **2012**, *66*, 54–60.

(24) Isogai, A.; Saito, T.; Fukuzumi, H. TEMPO-oxidized cellulose nanofibers. *Nanoscale* **2011**, *3*, 71–85.

(25) Scheirs, J.; Camino, G.; Tumiatti, W. Overview of water evolution during the thermal degradation of cellulose. *Eur. Polym. J.* **2001**, *37*, 933–942.

(26) Usov, I.; Nyström, G.; Adamcik, J.; Handschin, S.; Schütz, C.; Fall, A.; Bergström, L.; Mezzenga, R. Understanding nanocellulose chirality and structure–properties relationship at the single fibril level. *Nat. Commun.* **2015**, *6*, 7564.